Cyclic Elastic-Plastic Analysis of Pressure Vessel Components

A. Kalnins, D.P. Updike
Lehigh University, Dept. of Mechanical Engineering and Mechanics, Bethlehem, Pennsylvania 18015, U.S.A.

ABSTRACT

In some cases, pressure vessels are designed so that localized plastic strain appears. If the design pressure is maintained and some cyclic load, say temperature, superimposed, then it is important to know the status of the plastic zones as the cycling progresses, because plastic strain per cycle can be related to failure by low-cycle fatigue. This paper examines the plastic strain history for biaxial stress states that occurs in pressure vessels. Two examples, the knuckle region of a torispherical pressure vessel and the crotch region of two intersecting cylindrical shells, are examined in detail. The primary load in both cases is steady internal pressure. The cyclic temperatures are assumed to model the introduction of a hot fluid that is allowed to cool, then is heated up again, then cooled, and so on. We have shown that, depending on the temperature range, the knuckle region of the torispherical head can lead to shakedown or ratchetting. Whether or not a point can be reached at which the plastic straining settles down to a steady cycle was not determined in this paper, but will be pursued in further work. In the crotch region of intersecting cylindrical shells, the stress concentration at an unreinforced crotch produces severe plastic straining, and failure in a low number of temperature cycles is predicted.

INTRODUCTION

This paper is concerned with the failure of metals in low-cycle fatigue. Manson [1] and Coffin [2] have proposed that the basic cause of low-cycle fatigue is cyclic plastic strain that deteriorates the material until failure. Relatively few publications on fatigue in the presence of biaxial stress states are available. Relevant to this paper are those by Krempl [3], Brown and Miller [4], McDowell, et. al. [5], and Lawton [6].

ELASTIC-PLASTIC MODEL

We follow the established theory of plasticity and its application to axisymmetrically loaded shells of revolution. Except for the addition of kinematic strain hardening, our mathematical model is the same as that used by Marcal and Pilgrim [7]. We follow what is called "the stiffness method" of incremental plasticity. (For more references on this subject and its application to pressure vessels, see Chapter 8 of [8] by Kraus.)

Following the incremental theory of plasticity, the loading function is f, given by

$$f = \sqrt{(\sigma_\phi - c_1) + (\sigma_\theta - c_2) - (\sigma_\phi - c_1)(\sigma_\theta - c_2)} - Y \tag{1}$$

where σ_ϕ, σ_θ are the principal stress components (ϕ is the meridional and θ the circumferential angle of the axisymmetric reference surface); c_1,c_2 are the kinematic strain hardening parameters, representing the shift of the center of the von Mises ellipse; and Y gives the size of the ellipse. The problem is solved by incrementing loads, which produces increments in the stresses, $\delta\sigma_\phi$ and $\delta\sigma_\theta$, the total strains, $\delta\varepsilon_\phi$ and $\delta\varepsilon_\theta$, and the plastic strains, $\delta\varepsilon_{\phi p}$ and $\delta\varepsilon_{\theta p}$. During plastic straining, f=0, which leads to

$$\frac{\partial f}{\partial \sigma_\phi}\,\delta\sigma_\phi + \frac{\partial f}{\partial \sigma_\theta}\,\delta\sigma_\theta + \frac{\partial f}{\partial c_1}\,\delta c_1 + \frac{\partial f}{\partial c_2}\,\delta c_2 + \frac{\partial f}{\partial Y}\,\partial Y = 0 \tag{2}$$

We assume

$$\delta c_1 = \beta E_p[4(\delta\varepsilon_{\phi p}) + 2(\delta\varepsilon_{\theta p})]/3 \qquad \delta c_2 = \beta E_p[4(\delta\varepsilon_{\theta p}) + 2(\delta\varepsilon_{\phi p})]/3 \tag{3a}$$

$$\delta Y = (1-\beta)E_p\delta\varepsilon_{eqp} \qquad \delta\varepsilon_{eqp} = \frac{2}{\sqrt{3}}\sqrt{(\delta\varepsilon_{\phi p})^2 + (\delta\varepsilon_{\theta p})^2 + (\delta\varepsilon_{\phi p})(\delta\varepsilon_{\theta p})} \tag{3b}$$

which come from the of Prager-Ziegler kinematic strain hardening relationships and the Prandtl-Reuss theory. The value of β is adjusted to account for a combination of isotropic and kinematic strain hardening. E_p is the slope of a one-dimensional stress vs. plastic strain curve. Finally, the normality rule for the plastic strain increments requires that

$$\delta\varepsilon_{\phi p} = (\delta\lambda)\,\frac{\partial f}{\partial \sigma_\phi} \qquad \delta\varepsilon_{\theta p} = (\delta\lambda)\,\frac{\partial f}{\partial \sigma_\theta} \tag{4}$$

Upon unloading, f<0, and the elastic stress-strain relationships apply.

Substitution of (4) into (3), then into (2), determines $\delta\lambda$ in terms of $\delta\sigma_\phi$ and $\delta\sigma_\theta$. Putting it back into (4), adding the elastic and thermal strain increments, inverting, and adding to the stresses and strains at the beginning of the increment, leads to

$$\sigma_\phi = B_{11}\varepsilon_\phi + B_{12}\varepsilon_\theta + \tau_1 \qquad \sigma_\theta = B_{12}\varepsilon_\phi + B_{22}\varepsilon_\theta + \tau_2 \tag{5}$$

which are then integrated through the thickness of the shell to produce the shell stiffnesses. At this point, the boundary value problem is solved by the same technique that is used in the KSHEL programs [9].

ANALYSIS OF TORISPHERICAL PRESSURE VESSEL HEAD

The pressure vessel head chosen for investigation has the sharpest knuckle radius allowed by Division II of the ASME Pressure Vessel Code and no skirt before the transition from the head thickness of 2.00 in to the cylindrical shell thickness of 1.25 in. Figure 1 gives the geometry. The ASME Code gives a design internal pressure of 480 psi. Elastic-plastic analysis reveals that in the absence of residual stress an internal pressure of 480 psi produces a small plastic zone around point 14 (see Fig. 1). Purely elastic analysis reveals that a uniform temperature gradient of 202°F difference across the thickness produces initial yielding at point 22.

Consider the pressure vessel subjected to the design internal pressure of 480 psi and ask the question: how much plastic strain is produced by adding on to the pressure loading a cycle of heating and cooling of the fluid contained within the vessel? For this investigation, a peak temperature difference of 700°F across the wall is chosen with a uniform gradient through the wall. Material properties of the vessel are taken to be Young's modulus $E = 29 \times 10^3$ ksi, Poisson's ratio $\nu = 0.3$, coefficient of linear thermal expansion $\alpha = 6.5 \times 10^{-6}$ per °F, and yield stress $Y = 37$ ksi. Both strain hardening and dependence of yield stress on temperature are neglected.

Figures 2 and 3 show the path of the stress components at points 14 and 22, respectively, as the heating and cooling cycle takes place. Plastic straining can take place only when the path touches the von Mises ellipse, which is also plotted. On each figure, point A gives the stress components at the start of the cycle, point D gives the stresses at the reversing point where the temperature difference is 700°F, and point G gives the state where the temperature difference returns to zero. The tables accompanying Figures 2 and 3 give the values of temperature and the components of accumulated plastic strain corresponding to the points marked in the Figures. The path OK in Figure 2 shows the stress components of the elastic solution for temperature change of 202°F when the pressure is kept at zero.

Both stress paths shown indicate that the first cycle of thermal loading renders the stress state at the end of the full cycle different from that at the beginning of the cycle, thus, more than one load cycle must be treated to achieve a steady cyclic stress path. The stress for these additional cycles may be calculated in the same manner as for the first. The analysis of first thermal cycle shows the tendency of the stress paths to move toward a line of 45° slope, passing through the origin of the stress diagram. Thus, after several cycles, the active portions of the von Mises ellipses will be the portions of the sharp curvature where σ_ϕ and σ_θ are nearly equal. At the end of the heating cycle, both stresses are positive on the outer surface and negative on the inner surface. At the end of the cooling cycle the situation is reversed. The plastic strains thus will reverse during each cycle of loading, eventually leading to a low-cycle fatigue failure.

A comparison of the values of the plastic strain components (Figure 2) at the beginning and end of the cycle shows that the first cycle of thermal loading produces a net

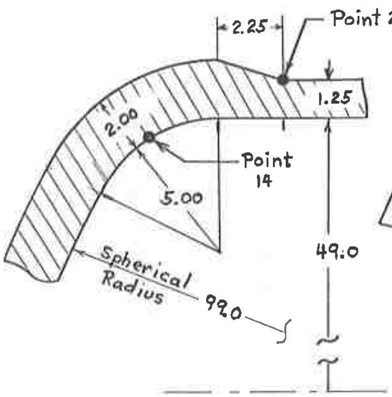

Figure 1. Geometry of Torispherical Head

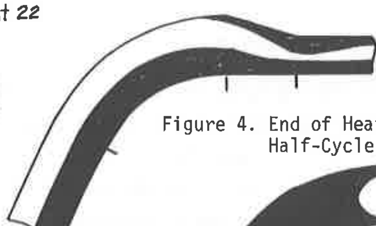

Figure 4. End of Heating Half-Cycle

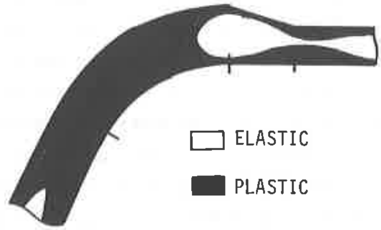

Figure 5. End of Cooling Half-Cycle

inward displacement in the knuckle region. The major part of this strain occurs as the stress path follows the path ABCD (Figure 2) along the von Mises ellipse. Due to the tendency of the cyclic stress path to move toward the 45° line through the origin of the stress plot with subsequent cycles of the thermal loading, the subsequent cycles will produce less and less inward displacement per cycle. This is because the early cycles produce a set of residual stresses favorable toward resisting the later cycles of thermal loading. The extent of the plastic zones is shown in Figures 4 and 5.

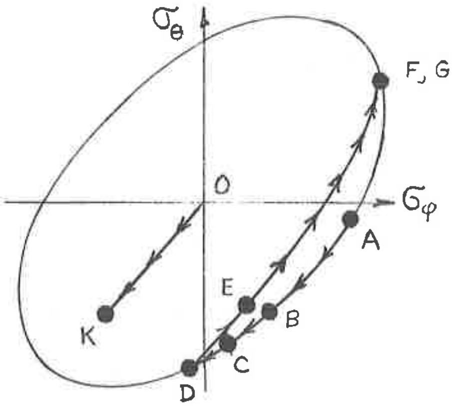

Point	Temp F°	$\epsilon_{\phi p}$ 10^{-3}	$\epsilon_{\theta p}$ 10^{-3}	ϵ_{eqp} 10^{-3}
A	0	0.35	-0.18	0.34
B	200	0.36	-0.19	0.35
C	300	0.55	-0.46	0.63
D	700	1.53	-2.34	2.51
E	600	1.53	-2.34	2.51
F	200	2.04	-2.19	3.09
G	0	5.06	-2.02	6.79

Figure 2. Stress Path and Plastic Strains at Point 14 in Knuckle

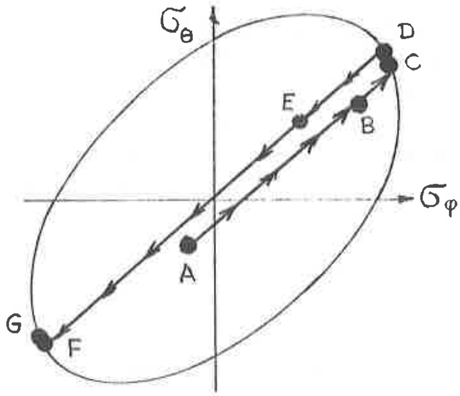

Point	Temp F°	$\epsilon_{\phi p}$ 10^{-3}	$\epsilon_{\theta p}$ 10^{-3}	ϵ_{eqp} 10^{-3}
A	0	0.00	0.00	0.00
B	200	0.00	0.00	0.00
C	300	0.22	0.09	0.33
D	700	2.26	1.38	3.73
E	600	2.26	1.38	3.73
F	200	1.59	1.00	4.80
G	0	-0.15	0.13	7.51

Figure 3. Stress Path and Plastic Strains at Point 22 in Transition

CROTCH REGION OF INTERSECTING SHELLS

In a series of previous papers, the authors have analyzed unreinforced intersections of equal diameter cylindrical shells subjected to internal pressure in the elastic [10], creep [11], and elastic-plastic range [12]. These analyses make use of an approximation, stemming from the fact that in the crotch region the solution varies rapidly in the direction along the cylinder generators and slowly along the circumference. The approximation reduces the problem to one of analysis of a shell of revolution subjected to axisymmetric loading. Using the same spirit of approximation in this paper, cycles of thermal gradient through thickness are superposed on the internal pressure loading. A radius-to-thickness ratio R/t = 100 is assumed and a Young's modulus to yield stress ratio of E/Y = 1000, so that the strain at initial yielding in a uniaxial test is $\epsilon_Y = 0.001$. The yield stress is taken as Y = 1000, so that all calculated stresses may be scaled to the yield stress Y by dividing by 1000. In the same manner, the calculated strains may be scaled to ε_Y by multiplying by 1000.

One problem is worked out in detail. First, an internal pressure of 1.5 times the pressure required to produce initial yielding is applied and held constant. This loading produces a contained plastic zone, extending from the crotch section into the shell. Then two and one-half cycles of thermal gradient loading are applied, the temperature difference across the wall thickness satisfying $E\alpha T/Y = 2$. This is the level of thermal stress required to just initiate yielding at the inner and outer surfaces of the cylinder in the absence of internal pressure. It is verified that a nearly steady stress cycle is achieved over the last full cycle of the thermal loading.

LIFE PREDICTION VARIABLES

When considering load cycles which produce a plastic strain change per cycle of the order of Y/E, as it occurs in the examples treated in this paper, the life prediction, or expected number of cycles to failure, must be based on the results of correlations of plastic strain per cycle, or per half-cycle, with the number of cycles to failure of test specimens. Of course, the test specimens are usually uniaxial specimens whereas thin-walled pressure vessels are biaxially stressed. For biaxially stressed materials, the equivalent plastic strain per cycle or half-cycle must be a function of cyclic changes of the two strain components, ε_ϕ and ε_θ. For this purpose several options are available for possible correlations with uniaxial fatigue data.

The first possibility is the accumulated equivalent plastic strain per cycle, given by

$$\Delta\varepsilon_{eq,p} = \Sigma\delta\varepsilon_{eq,p}$$

where $\delta\varepsilon_{eq,p}$ is called the equivalent plastic increment, defined by (3b), and the summation is carried out over a load cycle. Due to the radical in the above expression, the accumulated equivalent plastic strain can only increase over a cycle; therefore this parameter does not separate the strain contributing to accumulated dimensional change (ratchetting) from that of alternating plastic strain (fatigue). The computer program used here can calculate the above parameter at all points on the inner and outer surfaces of the vessel and plot it versus the position along the meridian. Figure 6 shows such a plot for the intersecting cylindrical shell problem.

Dimensional changes which occur over a full cycle of loading are given by the changes $\Delta\varepsilon_{\phi p}$ and $\Delta\varepsilon_{\theta p}$ in the plastic strain components. If purely alternating plasticity occurs, the quantities, $\Delta\varepsilon_{\phi p}$ and $\Delta\varepsilon_{\theta p}$, are zero; therefore $\Delta\varepsilon_{\phi p}$ and $\Delta\varepsilon_{\theta p}$ represent the ratchet strain per cycle. They cannot be used for low-cycle fatigue life predictions. They may, however, be used in life prediction if the failure criterion is one of allowable accumulated ratchet strain. Figure 7 shows the calculated components of ratchet strain per cycle for the cylindrical shell intersection problem. The components of ratchet strain per cycle may be used to compute an equivalent ratchet strain per cycle given by the following expression:

$$\text{equivalent ratchet strain per cycle} = [4[(\Delta\varepsilon_{\phi p})^2 + (\Delta\varepsilon_{\theta p})^2 + (\Delta\varepsilon_{\phi p})(\Delta\varepsilon_{\theta p})]/3]^{1/2}$$

Fatigue life predictions are based on the concept that the life of a structure correlate either with the total strain range or the plastic strain range. The strain range concept assumes that there is no accumulated or ratchet strain present. Therefore, in order to use the strain range concept in life predictions of vessels, undergoing a combination of alternating plasticity and ratchet straining, it is necessary to subtract out the ratchet components of the strain. The calculation may be performed as follows. Let g represent a variable, such as σ_ϕ, σ_θ, ϵ_ϕ, ϵ_θ, $\epsilon_{\phi p}$ or $\epsilon_{\theta p}$, for which the range is to be calculated. Let g_1 be the value of the variable at the beginning of the cycle, g_2 be its value at the half cycle or other load-reversal point, and g_3 be its value at the end of the cycle. The cycle must begin and end at a load-reversal point. The range of g is then defined as

$$g_2 - (g_1+g_3)/2$$

Figure 8 shows a plot of calculated components of strain range for the cylindrical shell intersection problem. Following the scheme used for ratchet strain components, the strain range components may be formed into an equivalent strain range. Figure 9 gives a plot of this variable for the inside surface of the cylinder intersection problem.

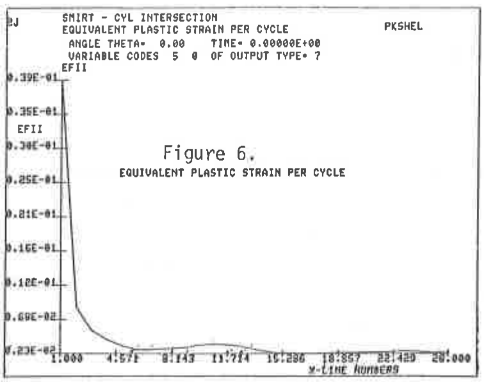

Figure 6.
EQUIVALENT PLASTIC STRAIN PER CYCLE

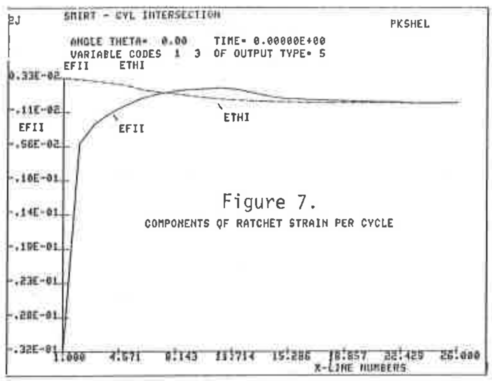

Figure 7.
COMPONENTS OF RATCHET STRAIN PER CYCLE

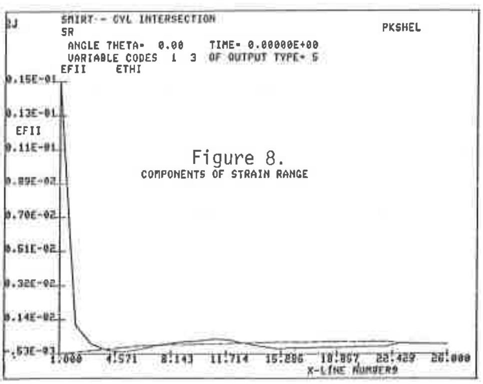

Figure 8.
COMPONENTS OF STRAIN RANGE

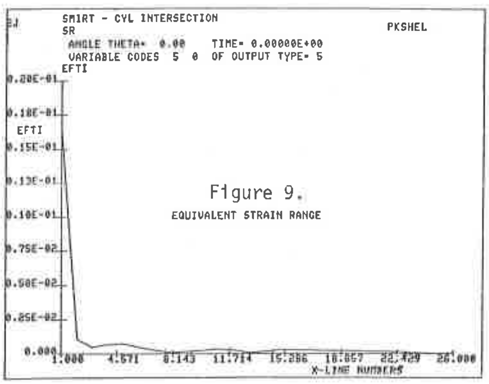

Figure 9.
EQUIVALENT STRAIN RANGE

DISCUSSION

Examination of Figures 6 , 7 , 8 , and 9 reveals that the highest plastic strains in the cylindrical shell intersection problem are due to the severe bending constraint right at the crotch point. If a shell is modeled as perfectly plastic, i.e., with no strain hardening, the possibility of a solution which contains plastic hinge circles certainly exists. Indeed, this is what is happening at the crotch point. The model predicts that at a plastic hinge-circle a finite change of slope occurs over a zero length of meridian of the shell. This implies an infinite curvature and an infinite bending strain. The very high strains predicted by the analysis reflect the model's attempt to achieve a plastic hinge-circle. Of course, the numerical analysis cannot predict an infinite strain, so it only predicts a very large strain.

A correct interpretation of a plastic hinge circle would be that the finite change of slope occurs over a length which is on the order of the shell wall thickness. Then the bending strain is on the order of the slope change. Shell theory must admit adding a short length on the order of the thickness so that the slope change can be distributed over that length. Such plastic hinge-circles may occur at concentrated ring loads, abrupt changes in meridianal direction, built-in edges, shell junctions, and abrupt changes in thickness or material. These are all cases for which the results of shell theory must be used with caution.

For the above reasons, we hesitate to make a life prediction for the crotch region using the peak strain calculated by shell theory.

REFERENCES

1. S.S. Manson, "Thermal Stresses in Design. Part 3", Machine Design, 1958, vol. 39, pp. 100-107.
2. L.F. Coffin, Jr., "A Study of the Effects of Cyclic Thermal Stresses in Ductile Materials", Transactions of ASME, 1954, vol. 76, pp. 931-944.
3. E. Krempl, "The Influence of State of Stress on Low-Cycle Fatigue of Structural Materials", ASTM STP 549, 1974.
4. M.W. Brown and K.J. Miller, "Two Decades of Progress in the Assessment of Multiaxial Low-Cycle Fatigue Life", ASTM STP 770, 1982, pp. 482-499.
5. D.L. McDowell, D.F. Socie, and H.S. Lamba, "Multiaxial Nonproportional Cyclic Deformation", ASTM STP 770, 1982, pp. 501-518.
6. C.W. Lawton, "Use of Low-Cycle Fatigue Data for Pressure Vessel Design", ASTM STP 770, 1982, pp. 585-599.
7. P.V. Marcal and W.R. Pilgrim, "A Stiffness Method for Elastic-Plastic Shells of Revolution", J. of Strain Analysis, 1966, vol. 1, pp. 339-350.
8. S.S. Gill, The Stress Analysis of Pressure Vessels & Pressure Vessel Components, Pergamon Press, 1970.
9. A. Kalnins, "Analysis of Shells of Revolution Subjected to Symmetrical and Nonsymmetrical Loads", J. Appl. Mech., 1964, vol. 86, pp. 467-476.
10. D.P. Updike and A. Kalnins, "Approximate Analysis of Intersecting Equal Diameter Cylindrical Shells Under Internal Pressure", J. of Pressure Vessel Techn., 1979, ASME Trans., vol. 101, pp. 194-199.
11. D.P. Updike and A. Kalnins, "Creep of Intersecting Equal Diameter Cylindrical Shells Under Internal Pressure", J. of Pressure Vessel Techn., 1983, ASME Trans. vol. 105, pp. 91-95.
12. D.P. Updike, "Approximate Elastic-Plastic Analysis of Intersecting Equal Dia. Cyl. Shells", J. Pres. Ves. Techn., 1981. vol. 103, pp. 111-115.